Geotechnical and Geophysical Site Characterisation 5 – Lehane, Acosta-Martínez & Kelly (Eds)
© 2016 Australian Geomechanics Society, Sydney, Australia, ISBN 978-0-9946261-1-0

Combined use of SDMT-CPTU results for site characterization and liquefaction analysis of canal levees

P. Monaco
University of L'Aquila – DICEAA, L'Aquila, Italy
L. Tonni, G. Gottardi & M. Marchi
University of Bologna – DICAM, Bologna, Italy
L. Martelli
Regione Emilia-Romagna, Servizio Geologico, Sismico e dei Suoli, Bologna, Italy
S. Amoroso
Istituto Nazionale di Geofisica e Vulcanologia, L'Aquila, Italy
L. Simeoni
University of Trento – DICAM, Trento, Italy

ABSTRACT: The paper illustrates the combined use of the results of seismic dilatometer tests (SDMT) and piezocone tests (CPTU), obtained as part of a comprehensive study aimed at investigating the post-earthquake stability conditions of canal levees damaged by the May 2012 Emilia (Italy) seismic sequence. The following issues are discussed: (1) Comparison of results obtained by SDMT vs. CPTU test interpretation, in particular soil type identification and ground property characterization of the embankment and the foundation soils. (2) Liquefaction analysis using a recent simplified method (Marchetti 2016) based on the combined use of the horizontal stress index K_D provided by SDMT and the cone penetration resistance q_t provided by CPTU. The results obtained by this method are compared with the results obtained by existing methods based on q_t (CPT) and K_D (DMT) alone, as well as with the results obtained by methods based on the shear wave velocity V_S and by laboratory cyclic tests.

1 INTRODUCTION

The seismic sequence which in May 2012 struck a wide area of the Po river plain (Emilia-Romagna region, Northern Italy) caused extensive damage to a number of riverbanks in the epicentral area, in the form of ground deformations, surface fractures and lateral spreading. Major damage was observed in a 3 km long segment of the embankment bordering an irrigation canal known as “Canale Diversivo di Burana” near Scortichino, Bondeno (Ferrara), hosting more than one hundred houses and productive activities. In some cases buildings and facilities built on the bank crown were found unstable or unsafe and thus declared unfit for use.

The municipality of Bondeno, supported by the Emilia-Romagna regional authority in cooperation with the Italian Geotechnical Society (AGI), promoted a Working Group of researchers from various Italian universities and experts of the Geological, Seismic and Soil Survey Regional Department, committed to analyzing the seismic response of the embankment, investigating the causes of the earthquake-induced damage, assessing the post-earthquake stability conditions and finally proposing remedial measures. A comprehensive site investigation program, including several in situ and laboratory tests, was performed for this task. The most significant results achieved by the Working Group activity were summarized by Tonni et al. (2015a). This paper is focused on the combined use of results from seismic dilatometer tests (SDMT) and piezocone tests (CPTU) for site characterization and liquefaction analysis.

2 SDMT-CPTU TESTS IN THE SCORTICHINO EMBANKMENT AREA

2.1 *Testing program and location*

The canal levee and the foundation soils were extensively investigated by in situ tests (5 boreholes, 12 CPTUs, 4 SDMTs, piezometer measurements, permeability tests) and by a large number of laboratory tests (triaxial, shearbox, resonant column and cyclic torsional shear, cyclic simple shear, double specimen direct simple shear) on undisturbed and reconstituted samples. Details on the test results and the relevant geotechnical parameters can be found in Tonni et al. (2015a,b). The site investigations were concentrated along cross-sections in four distinct areas (A, B, C, D, Fig. 1), located at about 1 km distance from each other, in which the most severe and extensive damages had been observed, particularly in the area C. In each investigated area (Fig. 2) at least three CPTU/SDMT soundings were carried out from the crest of the embankment, down to 30-35 m depth.

Figure 1. Aerial view of the damaged bank stretch and location of the investigated areas.

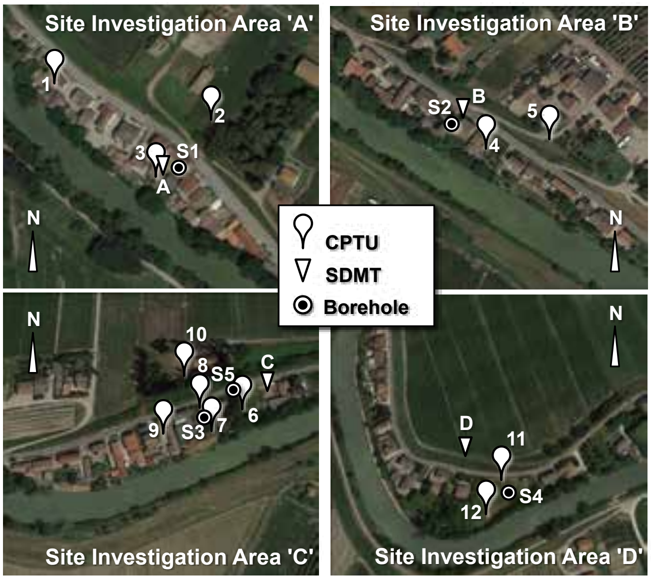

Figure 2. Location of in situ tests in the four selected areas.

2.2 *Interpretation of CPTU and SDMT results*

The borehole logs and the interpretation of CPTU and SDMT results (Tonni et al. 2015a,b) consistently allowed recognizing the following stratigraphic sequence and soil units from the crest of the embankment (see e.g. cross section c-c', area C, Fig. 3):

- an upper soil layer, about 9-10 m thick, composed of sandy silts and silty sands, corresponding to the core of the man-made embankment (Unit AR) in the topmost 6-7 m and to natural soils (Unit B) in the bottom portion;
- a clayey-silt layer with inclusions of peat and organic material (Unit C), generally ≈ 1-2 m thick;
- a medium to coarse or very coarse sand layer (Unit A) extending down to the maximum investigated depth, at least 40 m in thickness, locally including thin clayey lenses at depths between 30 and 34 m from the crest of the levee.

The above soil sequence was encountered in all the investigated areas, with minor variations in thickness of distinct soil units and/or in composition (predominantly sandy or silty) of Units AR and B. As an example, Fig. 4 shows the profiles of the corrected cone resistance q_t, the sleeve friction f_s and the pore pressure u provided by the piezocone test CPTU 6, carried out from the bank crest in area C. The plot also includes results from CPTU data interpretation, i.e. the profile of the Soil Behaviour Type (SBT), based on the Soil Behaviour Type Index I_{cn} calculated from the normalized cone resistance Q_{tn} and the normalized sleeve friction F_r (Robertson 2009), together with estimates of the friction angle φ' in each soil unit (Kulhawy & Mayne 1990 in coarse grained soil, Mayne & Campanella 2005 in fine grained soils) and of the undrained shear strength c_u in clays (Lunne et al. 1997).

Fig. 5 shows the results obtained from SDMT C, carried out from the bank crest in area C, in terms of profiles with depth of various parameters provided by usual DMT interpretation (Marchetti 1980, Marchetti et al. 2001), i.e. the material index I_D (indicating soil type), the horizontal stress index K_D (related to stress history/*OCR*), the constrained modulus *M*, the undrained shear strength c_u (in clay), the friction angle φ' (in sand), as well as the profiles of the measured shear wave velocity V_S and the small strain shear modulus G_0, obtained as $G_0 = \rho V_S^2$.

Both CPTU and SDMT profiles (Figs 4 and 5) denote rather poor mechanical properties of the soils in the upper ≈ 12 m below the crest of the embankment (Units AR, B and C). In particular the sandy-silty sediments of Unit B are characterized by low values of the horizontal stress index ($K_D \approx$ 1-2), which imply a low relative density D_R. Only the topmost 2-3 m of the embankment (Unit AR) show higher K_D values, presumably due to overconsolidation caused by desiccation-wetting cycles. The sands of Unit A, apart from sporadic thin layers having lower K_D, generally exhibit $K_D \approx$ 3-5, thus denoting a medium relative density ($D_R \approx 60\%$ according to Reyna & Chameau 1991). The interpretation of DMT results in the clay layers, excluding the shallow "crusts", indicates that the deposit is normally consolidated or slightly overconsolidated. The coefficient of earth pressure at rest in the fine-grained layers is generally $K_0 \approx$ 0.6-0.7.

V_S measured by SDMT (Fig. 5) increases gradually with depth from ≈ 150-200 m/s in the topmost soil layers to ≈ 300 m/s at about 35 m depth. The profiles of the constrained modulus *M* (Marchetti 1980) indicate high compressibility of Units AR, B, C ($M \approx$ 5-10 MPa) as well as of the deep clay layers, while the sands of Unit A are significantly less compressible. Differently from *M*, which refers to a "working strain" level (Marchetti et al. 2008), the values of the small strain shear modulus G_0, obtained from V_S measured in the same SDMT sounding, gradually increase with depth, without sharp contrasts between different soil layers.

The interpolation of the p_2 values measured by SDMT indicated the presence of two distinct groundwater levels, thus confirming measurements

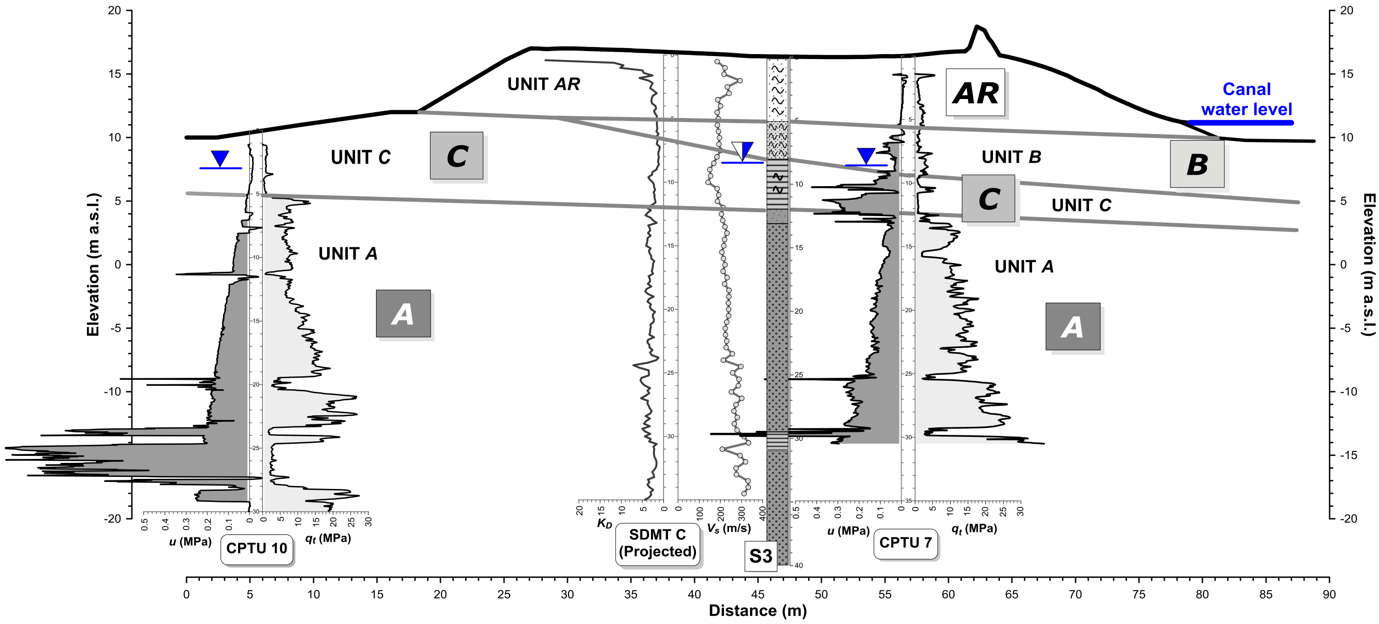

Figure 3. Stratigraphic model along the cross-section c-c', area C (Tonni et al. 2015a), including: borehole log; profiles of the corrected tip resistance q_t and the pore pressure u measured by CPTUs; profiles of the horizontal stress index K_D and the shear wave velocity V_S measured by SDMT.

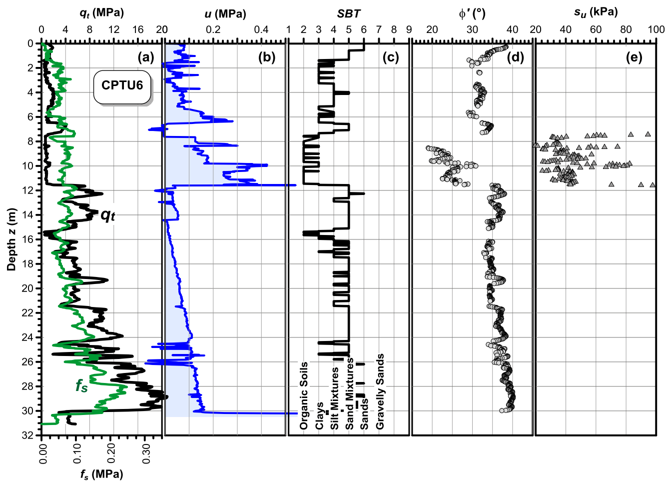

Figure 4. Interpretation of results of CPTU 6 (area C).

in open standpipe piezometers and existing wells: indeed, the upper level is located in the sandy-silty sediments of the embankment core (Unit AR) and the underlying Unit B, generally at 4-5 m depth from the crest, whilst a lower piezometric level, governing pore pressures in the confined sandy layer of Unit A (the so-called "Acquifero Padano") can be identified at about 7-8 m depth from the crest.

3 LIQUEFACTION ANALYSES

3.1 *Procedure and seismic input data*

Liquefaction analyses were carried out in each investigated area, in order to identify possible mechanisms responsible of the deformations and fractures observed on the crest of the embankment after the May 20, 2012 earthquake. The analyses were executed using a simplified dynamic approach, based on the comparison, at any depth, of the seismic demand on a soil layer generated by the earthquake (cyclic stress ratio *CSR*) and the capacity of the soil to resist liquefaction (cyclic resistance ratio *CRR*). When *CSR* is greater than *CRR* liquefaction may occur.

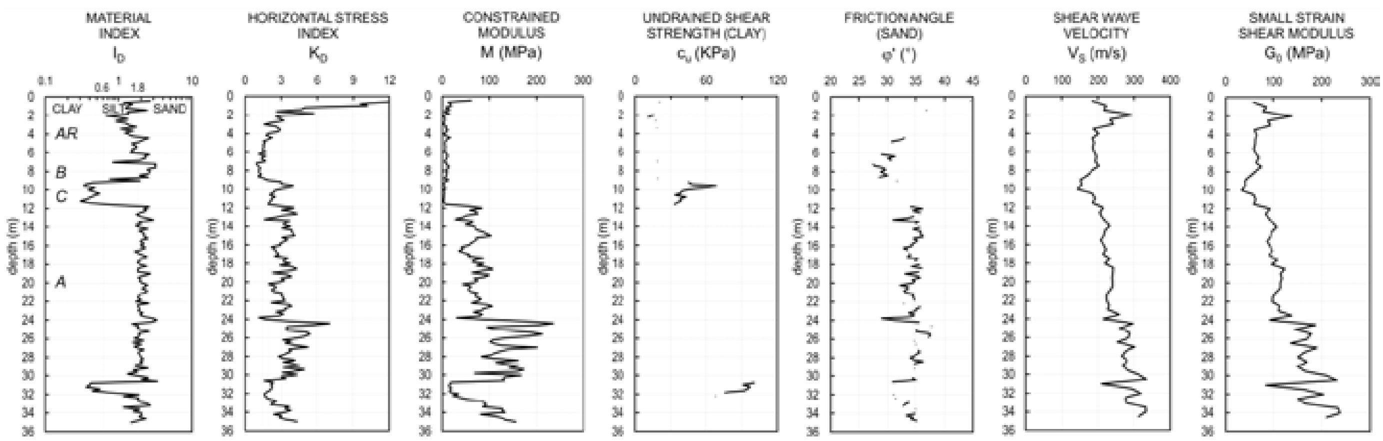

Figure 5. Interpretation of results of SDMT C (area C).

CSR was determined by 1-D ground seismic response analyses carried out using the code EERA (Bardet et al. 2000) in terms of total stresses, without taking into account the excess pore pressure build up typical of the liquefaction phenomenon. Details on the input data and results, obtained as part of the Working Group activity, can be found in Tonni et al. (2015a). The earthquake assumed as possible trigger of liquefaction was the May 20, 2012 main shock, recorded at 04:03 (local time), having local magnitude M_L = 5.9 and epicentral distance R_{epi} = 7.5 km from the Scortichino site. The main shock was followed, in about four minutes, by three aftershocks of M_L = 4.8, 4.8 and 5.0 respectively and by nine shocks having $M_L > 4$ within one hour. Since no ground motion recordings of this event were available in the area of Scortichino, the ground response analyses were carried out using four input accelerograms selected from the Italian earthquake database (ITACA 2011) by use of various search criteria (station on bedrock, moment magnitude M_w = 5.5-6.5, R_{epi} =5-10 km). In addition, a near-fault accelerogram obtained for the April 6, 2009 L'Aquila 2009 earthquake was also considered. All the input accelerograms were scaled to a peak ground acceleration PGA = 0.183 g, estimated using an attenuation law (Bindi et al. 2011).

At each depth *CSR* was evaluated as:

$$CSR = \frac{\tau_{av}}{\sigma'_{v0}} = \frac{0.65\tau_{\max}}{\sigma'_{v0}} \tag{1}$$

where τ_{max} is the maximum shear stress calculated by ground seismic response analysis (average of τ_{max} calculated using different accelerograms), τ_{av} = 0.65 τ_{max} is the amplitude of the shear stress of the equivalent regular sequence, and σ'_{v0} is the effective overburden stress at the given depth.

CSR was then compared with the cyclic resistance ratio *CRR* estimated by use of various methods based on the SDMT parameters V_S and K_D (Tonni et al. 2015b), on the cone penetration resistance q_t from CPTU and from laboratory cyclic simple shear tests (Tonni et al. 2015a). The liquefaction safety factor FS_{liq} at each depth was calculated as:

$$FS_{liq} = \frac{CRR}{CSR} = \frac{CRR_{M=7.5} \cdot MSF}{CSR} \tag{2}$$

where $CRR_{M=7.5}$ is the cyclic resistance ratio for a reference magnitude M_w = 7.5 (conventionally adopted in the simplified procedure) and *MSF* is a magnitude scaling factor. The analysis was carried out considering M_w = 6.14, equal to the maximum magnitude expected for a return period of 475 years in the seismogenetic zone in which Scortichino is located and similar to the magnitude of the May 20, 2012 main shock.

The "integral" liquefaction susceptibility at each test location was evaluated by means of the liquefaction potential index I_L (Iwasaki et al. 1982):

$$I_L = \int_{z=0}^{z_{crit}=20m} F(z) \cdot w(z)\,dz \tag{3}$$

where *w(z)* is a depth weighting factor and the function *F(z)* depends on the safety factor, according to Sonmez (2003).

3.2 *Evaluation of CRR from K_D (SDMT)*

In the last decades various *CRR*-K_D correlations have been developed, including the most recent shown in Fig. 6, which appear to converge towards a narrow central band. Results of liquefaction analyses based on K_D, with $CRR_{M=7.5}$ estimated according to Monaco et al. (2005), Tsai et al. (2009) and Robertson (2012), were presented by Tonni et al. (2015b).

3.3 *Evaluation of CRR from q_t (CPTU)*

Results of liquefaction analyses based on CPTU, with $CRR_{M=7.5}$ estimated from q_t according to Idriss & Boulanger (2004, 2006), were presented by Tonni et al. (2015a).

3.4 *Evaluation of CRR from the combination of K_D (SDMT) & q_t (CPTU)*

As noted by Marchetti (2016), much of the interest on the *CRR*-K_D correlation derives from the fact that the stress history increases significantly *CRR* and K_D, but only slightly the normalized cone resistance Q_{cn}. Hence it is possible that a correlation K_D-*CRR* will be stricter than Q_{cn}-*CRR*.

The *CRR*-K_D correlation recommended by Marchetti (2016), identified by the label "RIB" in Fig. 6, was defined by combining the Idriss & Boulanger (2004, 2006) *CRR*-Q_{cn} correlation (Eq. 4a):

$$CRR = \exp\left[(Q_{cn}/540) + (Q_{cn}/67)^2 - (Q_{cn}/80)^3 + (Q_{cn}/114)^4 - 3\right] \tag{4a}$$

and the Robertson (2012) average Q_{cn} - K_D interrelationship (Eq. 4b):

$$Q_{cn} = 25\,K_D \tag{4b}$$

A combined correlation for estimating *CRR* based at the same time on Q_{cn} and K_D (Eq. 5), plotted in the chart in Fig. 7 in the form $CRR = f\,(Q_{cn}, K_D)$, was obtained by Marchetti (2016) adopting as *CRR* the geometric average between a first *CRR* estimate obtained from Q_{cn} (Eq. 4a) and a second *CRR* estimate obtained from K_D (Eqs. 4a and 4b), namely:

$$\text{Average } CRR = [(CRR \text{ from } Q_{cn}) \cdot (CRR \text{ from } K_D)]^{0.5} \tag{5}$$

3.5 *Results and comments*

The results of liquefaction analyses based on different tests at the same location (area C) are compared in Fig. 8. The results provided by different methods

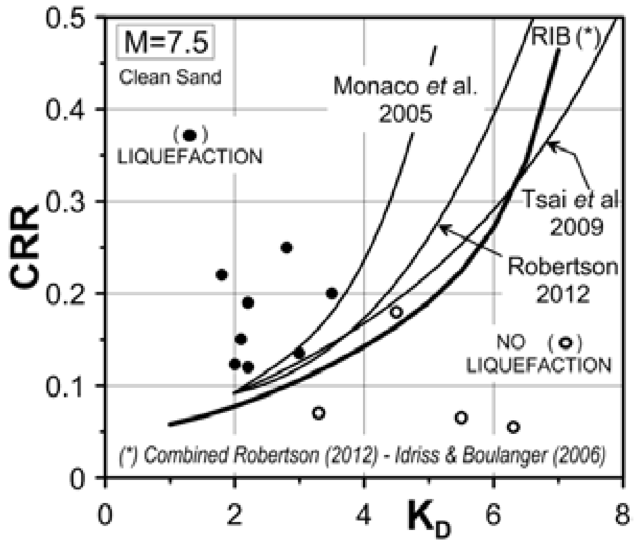

Figure 6. Recent *CRR*-K_D correlations (Marchetti 2016).

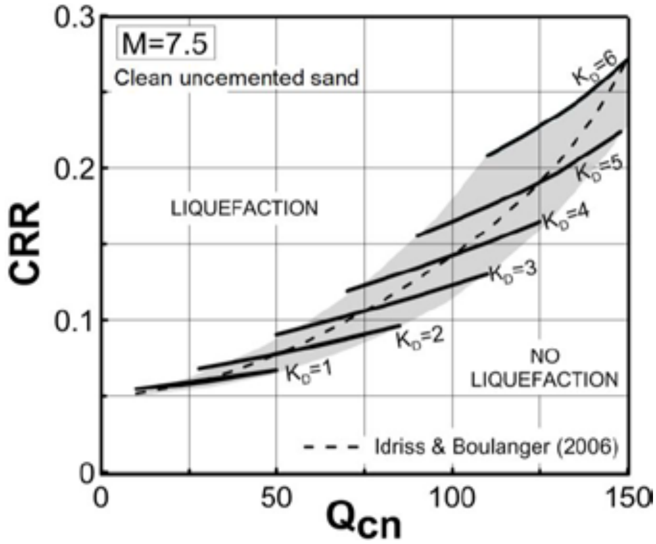

Figure 7. Correlation for estimating *CRR* based on both Q_{cn} and K_D, for clean uncemented sand (Marchetti 2016).

based on the DMT parameter K_D (Monaco et al. 2005, Tsai et al. 2009, Robertson 2012, Marchetti 2016 "RIB"), denoted by white symbols in Fig. 8, indicate possible occurrence of liquefaction (FS_{liq} < 1) in the silty-sandy soils at the base of the embankment (Unit B), at local depths from the crest between about 5 to 9 m, while no significant liquefaction is detected in the deeper sands (Unit A). The liquefaction potential index I_L estimated from K_D by all methods is "high".

The results of the analyses based on q_t from CPTU (Idriss & Boulanger 2004, 2006), denoted by black symbols in Fig. 8, signal the presence of a liquefiable layer, having much lower thickness than indicated by K_D, within the silty sand of Unit B. Differently from K_D, the analysis based on q_t suggests generalized liquefaction in the deeper sands (Unit A). The liquefaction potential index I_L is "moderate" to "high", i.e. lower than indicated by K_D.

The results obtained by the method proposed by Marchetti (2016), based on both K_D from SDMT and q_t from CPTU (grey symbols in Fig. 8), indicate the presence of a liquefiable layer of lower thickness than indicated by K_D alone within Unit B, in agreement with the analysis based on q_t alone. At the same time, this method tends to exclude significant liquefaction in Unit A, in agreement with the analyses based on K_D alone. The liquefaction potential index I_L is "low", i.e. substantially lower than indicated by methods based on both K_D and q_t alone.

To note that all the *CRR* correlations based on K_D (Monaco et al. 2005, Tsai et al. 2009, Robertson 2012, Marchetti 2016) are valid for clean sand, without any correction for fines content. Hence the *CRR* estimated from K_D in the sandy-silty layers (Units AR and B) are probably somewhat underestimated (though the low plasticity of fines in these layers should not involve a substantial increase in *CRR*), while in the clean sands of Unit A the *CRR* estimated from K_D are presumably realistic.

In Fig. 8 the results of the analyses based on K_D and q_t – alone and combined – are compared with the results obtained by Tonni et al. (2015b) using the correlations based on V_S by Andrus & Stokoe (2000) and Kayen et al. (2013). The analyses based on V_S generally indicate minor liquefaction ("low" I_L).

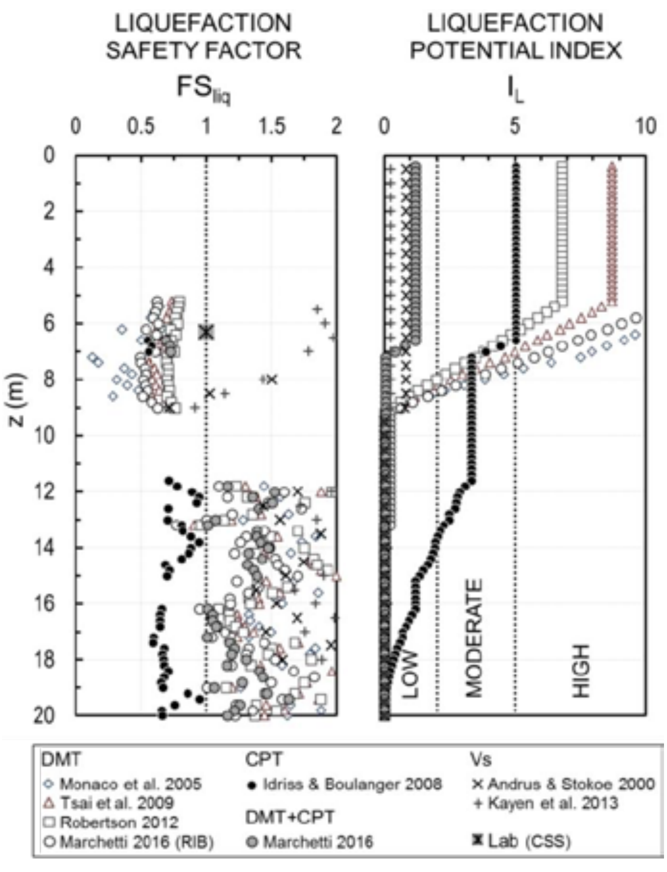

Figure 8. Area C. Results of liquefaction analyses based on the horizontal stress index K_D (SDMT), on the cone penetration resistance q_t (CPTU) and on the combination K_D (SDMT) & q_t (CPTU), compared with results obtained by methods based on the shear wave velocity V_S and by laboratory cyclic simple shear tests (CSS).

Fig. 8 also shows the value of FS_{liq} obtained by a laboratory cyclic simple shear test (CSS) performed on a silty-sandy sample taken in borehole S5 at 6.00-6.60 m depth. This result (FS_{liq} = 1) confirms the possible occurrence of liquefaction in the silty-sandy layer.

4 CONCLUSIONS

The results of liquefaction analyses carried out using simplified methods based on the DMT horizontal stress index K_D, in agreement with well-established methods based on the CPT cone penetration resistance q_t, suggest that plausibly local liquefaction phenomena, of variable extent, may have been induced by the May 20, 2012 earthquake in the sandy-silty soils below the Scortichino canal levee.

In the case illustrated in the paper, the use of a combined correlation for estimating *CRR* based at the same time on CPT-q_t and DMT-K_D (Marchetti 2016) has confirmed the probable occurrence of liquefaction. However the estimated overall liquefaction susceptibility, represented by the liquefaction potential index I_L, is lower than indicated by methods based on both K_D alone and q_t alone. This result is in reasonable agreement with field observations.

As noted by Marchetti (2016), it is expectable that an estimate based at the same time on two measured parameters is more accurate than estimates based on just one parameter, and incorporating the DMT stress history parameter K_D into the liquefaction correlations should possibly reduce the uncertainty in estimating *CRR*. Considerable additional research is obviously necessary, especially if the sand is not clean, uncemented sand.

5 REFERENCES

Andrus, R.D. & Stokoe, K.H., II. 2000. Liquefaction resistance of soils from shear-wave velocity. *J. Geotech. Geoenviron. Eng.*, 126(11): 1015-1025.

Bardet, J.P., Ichii, K. & Lin, C.H. 2000. EERA – A computer program for equivalent-linear earthquake site response analyses of layered soil deposits. Univ. Southern California.

Bindi, D., Pacor, F., Luzi, L., Puglia, R., Massa, M., Ameri, G. & Paolucci, R. 2011. Ground motion prediction equations derived from the Italian strong motion database. *Bull. Earthquake Eng.*, 9(6): 1899-1920.

Idriss, I.M. & Boulanger, R.W. 2004. Semi-empirical procedures for evaluating liquefaction potential during earthquakes. *Proc. 11th Int. Conf. on Soil Dyn. and Earthquake Eng. & 33rd Int. Conf. on Earthquake Geotech. Eng., Univ. of California, Berkeley*, 1: 32-56.

Idriss, I.M. & Boulanger, R.W. 2006. Semi-empirical procedures for evaluating liquefaction potential during earthquakes. *Soil Dyn. and Earthquake Eng.*, 26: 115-130.

ITACA 2011. ITalian ACcelerometric Archive (1972-2013), version 2.0, http://itaca.mi.ingv.it/ItacaNet/

Iwasaki, T., Tokida, K., Tatsuoka, F., Yasuda, S. & Sato, H. 1982. Microzonation for soil liquefaction potential using simplified methods. *Proc. 3rd Int. Conf. on Microzonation, Seattle*, 3: 1319-1330.

Kayen, R., Moss, R.E.S., Thompson, E.M., Seed, R.B., Cetin, K.O., Der Kiureghian, A., Tanaka, Y. & Tokimatsu, K. 2013. Shear-Wave Velocity-Based Probabilistic and Deterministic Assessment of Seismic Soil Liquefaction Potential. *J. Geotech. Geoenviron. Eng.*, 139(3): 407-419.

Kulhawy, F.H. & Mayne, P.W. 1990. Manual on estimating soil properties for foundation design. *Report EPRI EL-6800*, Electrical Power Research Institute, Palo Alto.

Lunne, T., Robertson, P.K. & Powell, J.J.M. 1997. *Cone Penetration Testing in Geotechnical Practice*. Blackie Academic & Professional, New York.

Marchetti, S. 1980. In Situ Tests by Flat Dilatometer. *J. Geotech. Eng. Div.*, 106(GT3): 299-321.

Marchetti, S. 2016. Incorporating the Stress History Parameter K_D of DMT into the Liquefaction Correlations in Clean Uncemented Sands. *J. Geotech. Geoenviron. Eng.*, 142(2): 04015072.

Marchetti, S., Monaco, P., Totani, G. & Calabrese, M. 2001. The Flat Dilatometer Test (DMT) in Soil Investigations – A Report by the ISSMGE Committee TC16. Official version approved by TC16 reprinted in *Flat Dilatometer Testing, Proc. 2nd Int. Conf. on the Flat Dilatometer, Washington D.C.*, 2006, Failmezger R.A. & Anderson J.B. (eds), 7-48.

Marchetti, S., Monaco, P., Totani, G. & Marchetti, D. 2008. In Situ Tests by Seismic Dilatometer (SDMT). *From Research to Practice in Geotechnical Engineering*, *Geotech. Spec. Publ. No. 180*, ASCE, 292-311.

Mayne, P.W. & Campanella, R.G. 2005. Versatile site characterization by seismic piezocone. *Proc. XVI ICSMGE, Osaka*, 2: 721-724.

Monaco, P., Marchetti, S., Totani, G. & Calabrese, M. 2005. Sand liquefiability assessment by Flat Dilatometer Test (DMT). *Proc. XVI ICSMGE, Osaka*, 4: 2693-2697.

Reyna, F. & Chameau, J.L. 1991. Dilatometer Based Liquefaction Potential of Sites in the Imperial Valley. *Proc. 2nd Int. Conf. on Recent Advances in Geotech. Earthquake Eng. and Soil Dyn., St. Louis*, 385-392

Robertson, P.K. 2009. Interpretation of cone penetration tests. A unified approach. *Canadian Geotech. J.*, 46(11): 1337-1355.

Robertson, P.K. 2012. The James K. Mitchell Lecture: Interpretation of in-situ tests – some insights. *Proc. 4th Int. Conf. on Geotechnical and Geophysical Site Characterization, Porto de Galinhas*, 1: 3-24.

Sonmez, H. 2003. Modification of the liquefaction potential index and liquefaction susceptibility mapping for a liquefaction-prone area (Inegol-Turkey). *Environ. Geology*, 44: 862-871.

Tonni, L., Gottardi, G., Amoroso, S., Bardotti, R., Bonzi, L., Chiaradonna, A., d'Onofrio, A., Fioravante, V., Ghinelli, A., Giretti, D., Lanzo, G., Madiai, C., Marchi, M., Martelli, L., Monaco, P., Porcino, D., Razzano, R., Rosselli, S., Severi, P., Silvestri, F., Simeoni, L., Vannucchi, G. & Aversa, S. 2015a. Interpreting the deformation phenomena triggered by the 2012 Emilia seismic sequence on the Canale Diversivo di Burana banks. *Rivista Italiana di Geotecnica,* XLIX(2): 28-58 (in Italian).

Tonni, L., Gottardi, G., Marchi, M., Martelli, L., Monaco, P., Simeoni, L. & Amoroso, S. 2015b. SDMT-based Site Characterization and Liquefaction Analysis of Canal Levees Damaged by the 2012 Emilia (Italy) Seismic Sequence. *Proc. 3rd International Conference on the Flat Dilatometer DMT'15, Rome, Italy*, 341-348.

Tsai, P., Lee, D., Kung, G.T. & Juang, C.H. 2009. Simplified DMT-based methods for evaluating liquefaction resistance of soils. *Engineering Geology*, 103: 13-22.